Int. J. Electrochem. Sci., 11 **(2016)** 3952 - 3962

International Journal of
ELECTROCHEMICAL
SCIENCE
www.electrochemsci.org

Short Communication

Investigation of the Consecutive Electron Transfer of Metalloporphyrin Species on the Simulative Cell Membrane by Thin Layer Cyclic Voltammetry

Wenting Gu[1,2], *Wenjian Li*[1,2], *Ruiyuan Liu*[1] *and Yin Qu*[1], *Libin Zhou*[1*],*Xicun Dong*[1,*]

[1] Institute of Modern Physics, Chinese Academy of Sciences, Lanzhou 730000, China
[2] School of Life Sciences, Lanzhou University, Lanzhou 730000, China
[3] Key Laboratory of Bioelectrochemistry&Environmental Analysis of Gansu Province, College of Chemistry & Chemical Engineering, Northwest Normal University, Lanzhou 730070, China
[*]E-mail: dongxicun@impcas.ac.cn, libinzhou@impcas.ac.cn

Received: 7 January 2016 / *Accepted:* 2 March 2016 / *Published:* 1 April 2016

Metalloporphyrin, which is the essential sites of electron transfer in biological system, can be investigated the electrochemical process on cell membrane. The liquid/liquid interface is suitable to simulate process of heterogeneous electron transfer between two immiscible electrolyte solutions by thin layer cyclic voltammetry conveniently. As the excellent electron receptors, metalloporphyrins obtained electrons from the electron donor $Fe(CN)_6^{4-}$, and the kinetics constants of multi-step interfacial bimolecular reaction were obtained simultaneously at the interface by thin-layer theory. Our experimental results suggested that the rate of electron transfer in the liquid/liquid interface depends on the presence of different metallic ions located the porphyrin ring. In addition, it is noted that the dependence of driving force on rate constants follows the well-known Bulter–Volmer equation. This electrochemical approach to quantitatively measure and analysis the dynamic process on cell membrane is a potential marker for the evaluation of electron transfer process in cell.

Keywords: Thin-layer cyclic voltammetry, Metalloporphyrin, Multi-step electron transfer, liquid/liquid interface

1. INTRODUCTION

Porphyrin derivatives are predominant over the essential biological processes, such as photosynthesis [1-4], dioxygen transport [5,6], and energy storage [7,8]. Recently, in order to gain insight into the essence of biological activity and physiological function in biological system, the main interesting has been focused on the studies of porphyrins[9-11]. In particular, porphyrin complexes

doi: 10.20964/110345

with various metallic ions in the porphyrin ring show some particular properties in the metabolism of living organisms due to their excellent electron-transfer properties, such as iron complex in the haemoproteins, magnesium complexes in the chlorophylls, and a cobalt complex in Vitamin B_{12}. It is vital for us to clarify the essence of many important physiological processes by exploring the mechanism of electron transport (ET) at the liquid/liquid interface of biological system. As novel applications of electrochemical field[9, 12-22], the liquid/liquid interface in biomembranes has been suggested as a simplified model for understanding the mechanism of electron transfer[22,36,39]. It has been recognized that electrochemistry is an efficient method to explore the process of electron transfer at the interface between two immiscible electrolyte solutions(ITLES)[23-27]. Particularly, the thin layer cyclic voltammetry(TLCV) developed by Anson et al. is characterized by simplicity and a limited amount of reactant.

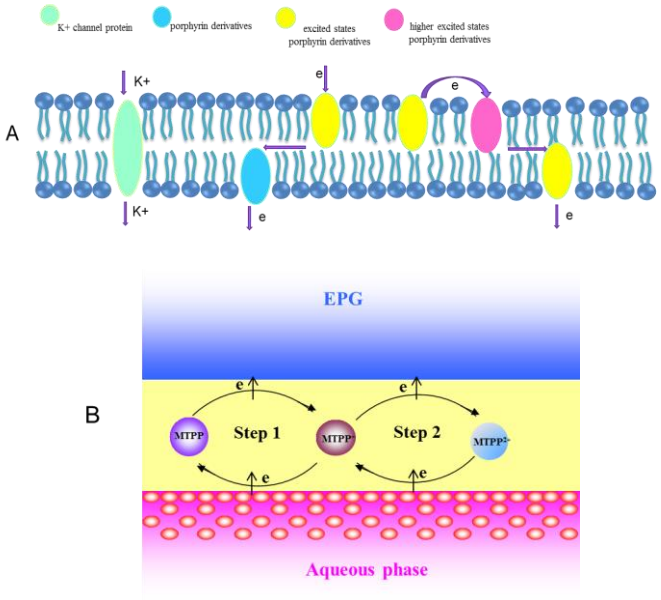

Scheme 1. (A) Schematic representations of two-step electron transfer process induced by porphyrin derivatives in cell membrane) and (B) Electrochemical reaction at the electrode.

Living systems are highly complex samples involving not only single ET but also multi-step ET in nature. To date, there are a great deal of reports the effect of driving force on the measured ET at liquid/liquid interface[25, 28-30]. Particularly, the obtained kinetic data could explain the dependence of the redox couples in the aqueous phase on porphyrin in the organics phases[11]. The results were in good agreement with Marcus theory: for the low driving force, the rate satisfies Bulter-Volmer kinetics, i.e., the rate increases as the driving force increases; for the high driving force, the Marcus inverted region kinetics has been observed[31-33]. By the thin layer cyclic voltammetry, many reactant pairs have been observed in the work of Shi and Anson[25]. It is also noted from the result that the rates is nearly sensitivity to the driving force. Much attention has been focused on the dependence of the rate of interfacial ET processes on the driving force of the interface reaction[11,30,34]. However, few

papers have studied the electron transfer of metalloporphyrins in the transition metal elements across the ITIES by TLCV in this field.

In this paper, in order to investigate the effect of metabolic processes, which provides the important guideline for the biological activity and physiological function, the metalloporphyrins with different metallic elements in transition metal elements were implemented at the nitrobenzene/water (NB/W) interface based on the electrochemical method by TLCV. Due to the excellent complexing properties and strong redox activity, metalloporphyrins in transition metal elements can be used to simulate ET in biological cell[29,30,35]. Our obtained results have shown that the rate of interfacial ET processes strongly depend on the presence of different metallic ions in the porphyrin complexes. These studies could help us clarify the mechanism of electron transfer in metal transition series elements, also expose the molecular mechanism in biological cell.

2. EXPERIMENTAL

2.1. Chemicals and apparatus

NaCl, $NaClO_4$, $K_4Fe(CN)_6$ (AR, Beijing Chemical Reagent Co.), nitrobenzene (NB) (Shanghai Chemical Reagent Co. Ltd.), were of highest available purity, they were used as received. Tetrabutylammonium perchlorate ($TBAClO_4$) was synthesized in our lab according to the Ref. 41. 5,10,15,20-Tetraphenyl porphyrin iron (FeTPP). 5,10,15,20-tetraphenyl porphyrin cobalt (CoTPP) and 5,10,15,20-tetraphenylporphyrin nickel (NiTPP) were provided[28]. The present experiments were implemented in CHI-832 working station (CHI instrument, Co. Ltd., Austin, USA) by thin-layer cyclic voltammetry and cyclic voltammetry. A three-electrode configuration (EPG, auxiliary and reference) was applied throughout our experiments. The edge-plane pyrolytic graphite electrodes (EPG) with 0.3 cm^2 of the edges of the graphite planes was prepared. Both Pt counter electrode and Ag/AgCl: KCl reference electrode were also used. The experiments were implemented at the room temperature (22±2°C).

2.2. Procedures

The EPG was pretreated as described [23]. The resulting surface was moderately hydrophobic as indicated by the failure of a drop of water to spread across its surface. When thin layers of NB solutions containing interest reactants (FeTPP, CoTPP and NiTPP) and supporting electrolytes ($TBAClO_4$) were applied to the graphite electrode held in an upside-down position by transferring 1.5μL of the solutions to the electrode surface with a microsyringe, the organic liquid spread spontaneously across the surface of the graphite electrode. The electrode was then turned over and immediately immersed in the aqueous solution.

3. RESULTS AND DISCUSSION

In the present paper, both the metalloporphyrin in the NB phase and redox species in the aqueous phase are investigated to explore the biological activity and physiological function of natural

compounds on the simulative cell membrane based on the TLCV. In Scheme 1A, the primary process of two-step electron transfer in cell membrane is shown. The porphyrin derivatives was reduced by reductive enzyme and gained one electron to form excited-state which move inside and outside the cell membrane, and transfer electrons to redox species, while some of the excited-state porphyrin derivatives again gained one electron to higher excited states porphyrin derivatives which was oxidized on cell membrane similarly. Up to here, a full consecutive electron transfer was completed and the system achieved the purpose of energy transfer. The intricate reactions could be simulated simply by electrochemical reaction at the electrode as shown in Scheme 1B. At first, the MTPP is oxidized to $MTPP^+$ on the electrode. One part of $MTPP^+$ could diffuse to the liquid/liquid interface and occur redox-active reactants and gain an electron from the $Fe(CN)_6^{4-}$, and restore into MTPP. Then, MTPP diffuse to the electrode, and the first feedback current is captured by the electrode when the first step ET process was finished. Meanwhile, other $MTPP^+$ will be continually oxidized to $MTPP^{2+}$ due to the reduction of $Fe(CN)_6^{4-}$ at the interface. The electrochemical reactions are given as follows:

$$MTPP \xrightarrow{-e} MTPP^+ \xrightarrow{-e} MTPP^{2+}(EPG) \quad (1)$$

$$MTPP^+ + Fe(CN)_6^{4-} \longrightarrow MTPP + Fe(CN)_6^{3-}(ITIES) \quad (2)$$

$$MTPP^{2+} + Fe(CN)_6^{4-} \longrightarrow MTPP^+ + Fe(CN)_6^{3-}(ITIES) \quad (3)$$

where M represents the group of Fe, Co and Ni in the porphyrin ring, respectively.

3.1. Electron transfer from metalloporphyrins with various metallic ions to $Fe(CN)_6^{4-}$ across the NB/H_2O interface

In Fig. 1, the reversible cyclic voltammogram (CV) of iron porphyrin (FeTPP) is shown in NB phase with supporting electrolyte of 10mM $TBAClO_4$. As one can see, one-electron wave can be clearly observed, which means that one electron oxidation reactant occur between Fe(II)TPP and Fe(III)TPP. It is noted that a typical steady-state voltammogram with two well-defined waves indicates the process of two-step one-electron oxidations between CoTPP and NiTPP. Iron(II) porphyrin was oxidated to iron(III) porphyrin at EPG and then was diffused to the liquid/liquid interface, which plays a role of the simulated membrane in the present experiment. However, in the two-step one-electron oxidations, CoTPP can be oxidated to $CoTPP^+$ and $CoTPP^{2+}$. At the same time, the similar results were also observed in NiTPP (shown in Fig.1). Compared with that of FeTPP, it is noted that the redox potential of NiTPP has an apparent positive shift, while a negative shift can be observed for CoTPP. As one can also see in Fig.1, the electrode process depends on the presence of the different metallic ions in the three types of metalloporphyrins. Due to the decreased density of electron cloud of the porphyrin rings, NiTPP will be oxidized at a more positive potential. The result is consistent with the Abdul Wahab[36].

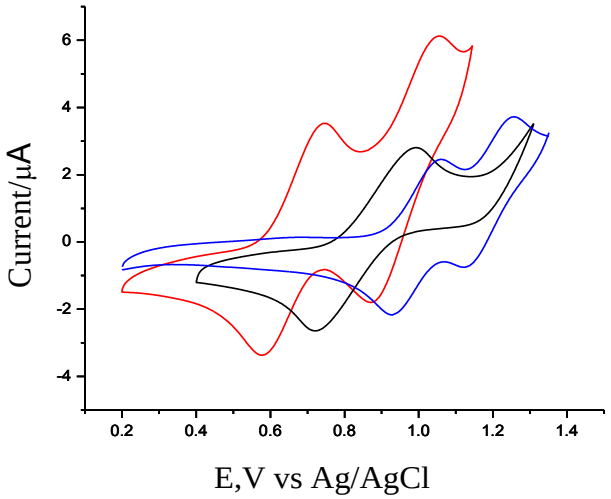

Figure 1. Steady-state cyclic voltammogram of three types of metalloporphyrins (from left to right: 1mM CoTPP, 1mM FeTPP, 1mM NiTPP, supporting electrolyte of 0.01 M $TBAClO_4$). Scan rate of 5 mV s^{-1}.

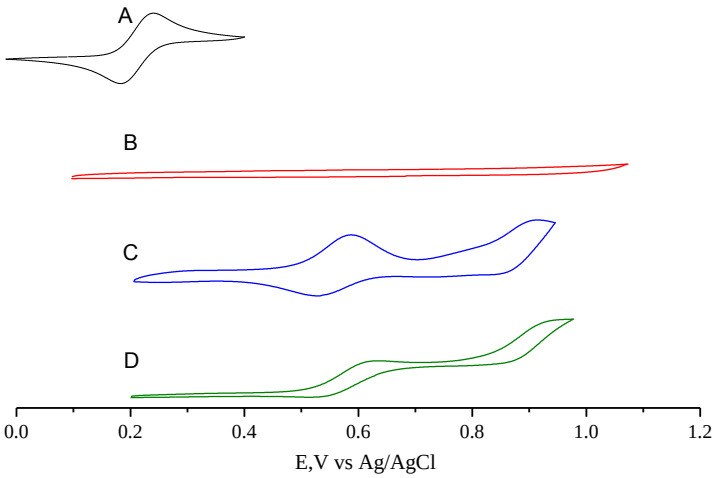

Figure 2. Thin-layer cyclic voltammogram of electron transfer between CoTPP and $K_4Fe(CN)_6$ for (A) 10 mM $K_4Fe(CN)_6$ at an uncoated EPG electrode with the supporting electrolyte of 0.1 M $NaClO_4$ + 0.1 M NaCl, (B) Repeat of part A after the electrode surface was covered with NB of 1.5μL, (C) the electrode covered with NB of 1.5μL, 1 m MCoTPP, and supporting electrolyte (0.01 M $TBAClO_4$). The aqueous solution contained only supporting electrolyte (0.1 M $NaClO_4$ + 0.1 M NaCl). (D) Repeat of part C with 10 mM $K_4Fe(CN)_6$ present in the aqueous phase; 1.5μL of NB containing 1 mMCoTPP and supporting electrolyte (0.01 M $TBAClO_4$). Scan rate of 5 mV s^{-1}. The inset shows the cyclic voltammogram obtained at the EPG electrode with the solution of NB cotaining 1mM CoTPP and 0.01 M $TBAClO_4$.

The above mentioned phenomena owing to the different molecular configurations of metalloporphyrins in transition metal elements. It can be concluded that the process of electron transfer depends on the presence of different metal elements in the porphyrin rings. It can be also inferred that the redox potential of the metalloporphyrins can be affected by the central metal elements[37]. Such a

large formal potential difference plays an important role in the studies of electron transfer kinetics across an ITIES.

In Fig. 2A, we have presented a cyclic voltammogram recorded at a bare edge plane EPG electrode in a 10 mM aqueous solution of $Fe(CN)_6^{4-}$ with the supporting electrolyte of 0.1 M $NaClO_4$+ 0.1 M NaCl. When a thin layer of NB was fixed on the electrode surface to separate it from the aqueous solution, no voltammetric current was obtained for the oxidized reactant. The phenomena can be explained that any form of $Fe(CN)_6^{4-}$ ions incapably reach the electrode surface (shown in Fig.2B). Both CoTPP and 0.01 M $TBAClO_4$ supporting electrolyte were dissolved in the NB when the thin layer was observed on the electrode with only supporting electrolyte for the aqueous solution. The corresponding response is shown in Figure 2C. As one can see, the anodic currents are enhanced at the potential. Meanwhile, CoTPP and $CoTPP^+$ will be formed due to the presence of $CoTPP^+$ and $CoTPP^{2+}$. It is inferred that cross-phase electron transfer will be observed from CoTPP to $Fe(CN)_6^{4-}$ in the aqueous phase. The two couples near 0.75 and 1.05 are the apparent half-wave potential of the $CoTPP^+$/ CoTPP, and $CoTPP^{2+}$/ $CoTPP^+$ couple, respectively. In order to verify the stable phenomena, we have repetitive scanned between +1.1 and -0.1 V and found that the tendency of decrease can exist still in the peak currents. Thus, the difference between the formal potentials of the two reactants, ΔE, can be obtained. In the combination of $Fe(CN)_6^{4-}$ and the aqueous phase, repeating the operation shown in Fig. 2C, the anodic plateau can occur as shown in Fig.2D. It is concluded that the steady-state can be obtained by the biomolecular redox reaction. The obvious potential difference is interesting on the study of ET kinetics across an ITIES[25]. As well-known, every cycle of life will be related to the process of multistep ET. In order to clarify the processes of ET, scanning electrochemical microscopy (SECM) was used to investigate the process of electron transfer. However, it is noted that the results obtained by SECM are essentially indistinguishable from the consecutive ET when single step ET is analyzed by the mode of feedback[30].

3.2. Theoretical Analysis for Consecutive Interfacial Electron Transfer

In order to qualify the rate constant of bimolecular reaction at the liquid/ liquid interface, i_{obs} should be measured for several concentrations of aqueous phase without change of organic phase[22,24-27,38,39]. In the manipulation, when the concentration of $Fe(CN)_6^{4-}$ is sufficiently high in the aqueous phase, the concentration of CoTPP will be neglected at the NB/H_2O interface. Meanwhile, the cathodic plateau cuurent i_D can be affected by the diffusion mechamism of CoTPP and CoTPP+. However, for a stable concentratrion of CoTPP and CoTPP+, the concentrations of $Fe(CN)_6^{4-}$ will be varied from 10 to 40mM (shown in Fig. 3). It is noted from the fitted curve that i_{obs} is independent when the concentration of $Fe(CN)_6^{4-}$ is surricently high in the aqueous phase. Based on Eqs. 5 to 9, the dependence of i_{obs} on $C_{Fe(CN)6}^{4-}$ is shown in Fig. 3, respectively. The corresponding rate constants are obtained and listed in Table 1.

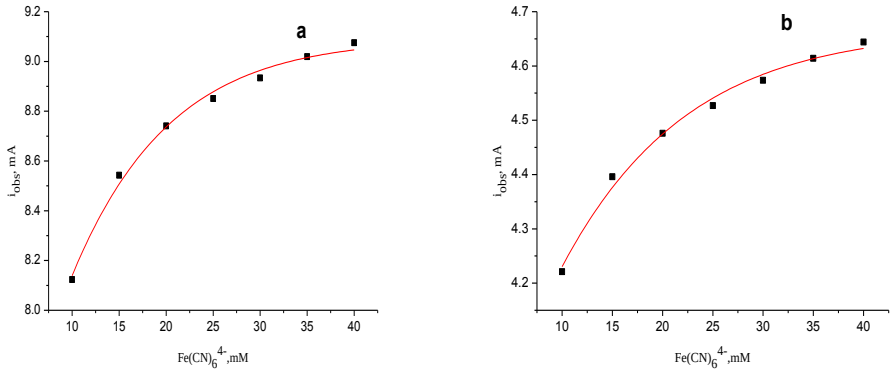

Figure 3A (a) Dependence of the steady-state currents (i_{obs}) of the first step ET on the concentration of $K_4Fe(CN)_6$ in the aqueous phase (b) Dependence of the steady-state currents (i_{obs}) of the second step ET on the concentration of $K_4Fe(CN)_6$ in the aqueous phase.

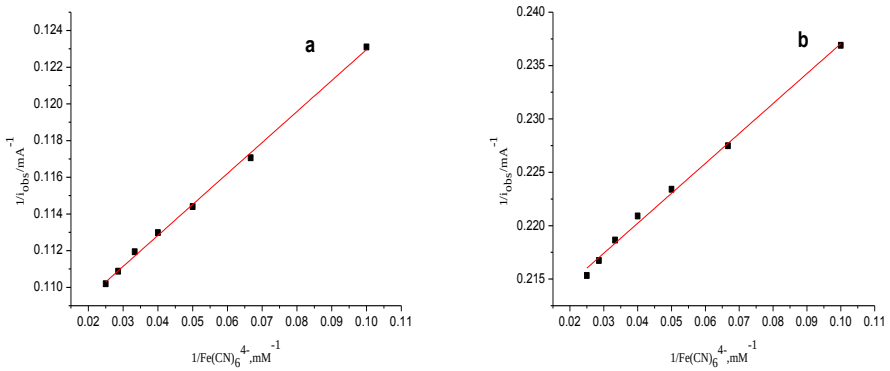

Figure 3B Dependence of reciprocal observed currents on $[K_4Fe(CN)_6]^{-1}$ (a) for the first step ET and (b) for the second step ET.

According to these conditions, the rate constant of the first step ET can be obtained by the TLCV analysis theory [23-27]. An expression 8 can be derived from Eqs.5, 6 and 7.

$$\frac{1}{i_{obs}} = \frac{1}{i_D} + \frac{1}{i_{ET}} \quad (5)$$

$$i_D = nFAc^*_{NB}D_{NB_1}/d \quad (6)$$

$$i_{ET} = nFAk_{et}c^*_{NB}c^*_{H_2O} \quad (7)$$

$$(i_{obs})^{-1} = d/(nFAc^*_{NB}D_{NB}) + (nFAc^*_{NB})^{-1}(c^*_{H_2O})^{-1}k_{et}^{-1} \quad (8)$$

Where c^*_{NB} and c^*_{H2O} are the initial bulk concentration of reactant contained in organic phase and dissolved in the aqueous phase, respectively. k_{et} is the bimolecular rate constant for the redox reaction at the interface between two immiscible electrolyte solutions. d is the thickness of thin layer. n is the number of electrons transfer. F is Faraday's constant. A is the area of electrode area. D_{NB} is the diffusion coefficient of reactant in the organic. i_D is the steady-state limit-diffusion current. i_{ET} is the characteristic current corresponding to the electron-transfer process across the phases. i_{obs} is the

observed plateau current. The dependence of $(i_{obs})^{-1}$ on $(c_{H2O})^{-1}$ should be linear with a slope $(nFAc^*_{NB}k_{et}^{-1})$. Thus, we can calculate k_{et} with intercept of $(i_D)^{-1}$.

However, it is noted that with the achievement of each step ET, the concentration of reactant in organic phase for the subsequent step ET will be gradually varied. Thus, for the multi-step cross-phase electron transfer reaction, our main attention is focused on the measure of the concentration of reactant in the organic phase for the following step ET. It is clearly cognized that the concentration of organic species in the following step is affected by the initial bulk concentration of reactant dissolved in the organic phase. According to Eq.6, the ratio of diffusion-controlled current (i_D) of voltammetric response is determined under steady-state conditions. We assume that the concentration of c^*_{NB1} for the first step is constant and equals to the initial value. i_{D1} and i_{Dn} can be obtained from the intercept of dependence of $(i_{obs})^{-1}$ on $(c_{H2O})^{-1}$. The concentration for the subsequent step is given as follows,

$$\frac{i_{D_1}}{i_{D_n}} = \frac{c^*_{NB_1}}{c^*_{NB_n}} \quad (n>1) \qquad (9)$$

$$c^*_{NB_n} = \frac{i_{D_n}}{i_{D_1}} \times c^*_{NB_1}$$

Thus, for the multi-step ET, Eqs. (9) could be used to calculate the concentration of the organic species for the following step.

Table 1. Rate constants of bimolecular for single-step and two-step cross phase electron transfer

	Redox species In the organic phase[a]	E^f_{H2O} mV[b]	E^f_{NB}mV[c]	Overall driving force (mV)[d]	k_{et} cms^{-1} M^{-1}
I	CoTPP	222	695	457	0.068
II	CoTPP	222	1053	815	0.0895
I	FeTPP	222	810	572	0.04115
I	NiTPP	222	620	382	0.03255
II	NiTPP	222	959	721	0.04493

a Redox species of the organic phase.

b Formal potential of the reactant redox couple in the H_2O phase vs a saturated Ag/AgCl electrode

c Apparent formal potential of the reactant redox couple in the NB phase vs a saturated Ag / AgCl electrode in the H_2O phase

d The overall driving force of the reaction: $(E^f_{H2O} - E^f_{NB})$.

3.3. Dependence of driving force on the rates of ET at the ITIES

The overall driving force is defined by the difference between the formal potentials of the two redox couples in their respective phases and $\Delta_w^0\phi$, the Galvani potential difference at the liquid/liquid

interface. The overall driving force can be considerably changed by using the different redox couples either in the aqueous phase, or in the organic phase. It is desirable for TLCV measurement of rapid ET kinetics at ITIES to investigate the processes of the electron transfer. Besides, the traditional studies of charge transfer on liquid/liquid interface can also be used to display the dependence of different metallic ions on the molecules of metalloporphyrins in transition metal elements.

The driving force will increase when the organic phase reactant varies. However, the concentrations of the potential of ClO^-_4 in the two phases are constants. According to Marcus theory [33], the k_{et} of the bimolecular rate constant k_{et} is described by the following equations,

$$k_{et} = const \exp(-\Delta G^{\neq} / RT) \quad (10)$$

$$\Delta G^{\neq} = (\lambda / 4)(1 + \Delta G^0 / \lambda)^2 \quad (11)$$

$$\Delta G^O = -F(\Delta E^0 + \Delta^o_w \phi) \quad (12)$$

where $\Delta G^{\neq}$ is the free energy of activation. ΔG^0 is the standard free energy of reaction i.e., the driving force in Liquid/liquid interface. Due to the presence of different metallic ions, regulate the driving force for the ET reaction can be regulated in our experiment. Things will be interesting once the bimolecular rates k_{et} shown in Table1 are obtained according to Eqs.10. Based on Marcus theory, the rate constant satisfies Bulter–Volmer kinetics, where the rate increases as the increase of driving force for the low driving force. At the high driving force, the rates will decrease. The phenomena are in good excellent with Marcus inverted region [31-33]. In the present paper, it is noted that the dependence of rate constant on the driving force can be controlled by the regulation of metallic ions of porphyrin complex in transition metal elements. As one can see from Table 1, the rate constants increase with the increase of the driving force, which indicates that the dependence of k_{et} on the overall driving force for the consecutive ET is in good agreement with the conventional Butler-Volmer treatment[40,41].

4. CONCLUSIONS

In this paper, in order to explore the effect of metabolic processes in a biological system, the metalloporphyrins that containing different metallic elements in transition metal elements were used to survey the biological and physiological function of compounds at the nitrobenzene/water (NB/W) interface by the electrochemical method of TLCV. The obtained results have indicated that the rate of interfacial ET processes depend on the presence of different metallic ions in the porphyrin complexes, and follows Bulter–Volmer kinetics in certain range. These studies provide some significance and help us explain the molecular mechanism of biological system in nature.

ACKNOWLEDGEMENTS

This work was supported by the STS project (KFJ-EW-STS-086), National Natural Science Foundation of China (11575259), Youth Innovation Promotion Association of Chinese Academy of Sciences (CAS) (29Y506030) and Western Light Co-scholar (29Y406020, 29Y506020) Program of CAS, and the Key Laboratory of Polymer Materials of Gansu Province of China. Wenting Gu thanks Prof. Xiaoquan Lu for help discussions at College of Chemistry & Chemical Engineering, Northwest Normal University.

References

1. M. Fujitsuka, M. Hara, S. Tojo, A. Okada, V. Troiani, N. Solladié, T. Majima, *J. Phys. Chem. B.*, 109 (2004) 33-35.
2. B. Munge, S. K. Das, R. Ilagan, Z. Pendon, J. Yang, H. A. Frank, J. F. Rusling, *J. Am. Chem. Soc.*, 125 (2003) 12457-12463.
3. X. Peng, N. Aratan, A. Takag, T. Matsumoto, T. Kawai, I-W. Hwang, T. K. Ahn, D. Kim, A. Osuka, *J. Am. Chem. Soc*., 126 (2004) 4468-4469.
4. F. Longobardi, P. Cosma, F. Milano, A. Agostiano, J. Mauzeroll, A. Bard, J. *Anal. Chem.*, 78 (2006) 5046-5051.
5. Goldberg, D. P., *Acc. Chem. Res*., 40 (2007) 626-34.
6. I. Hijazi, T. Roisnel, P. Even-Hernandez, E. Furet, J.-F. o. Halet, O. Cador, B. Boitrel, *J. Am. Chem. Soc.*, 132 (2010) 10652-3.
7. C. Hu, B. C. Noll, C. E. Schulz, W. R. Scheidt, *Inorg. Chem*., 47 (2008) 10984-91.
8. R. Ricoux, R. Dubuc, C. Dupont, J.-D. Marechal, A. Martin, M. Sellier, J.-P.Mahy, *Bioconj. Chem.*, 19 (2008) 899-910.
9. M. Biesaga, K. Pyrzyska, M. Trojanowicz, *Talanta*, 51 (2000) 209–224.
10. M. T. Barton, N. M. Rowley, P. R. Ashton, *J. Chem. Soc., Dalton Trans*., (2000) 3170–3175.
11. Z. Ding, B. M. Quinn, A. J. Bard, *J. Phys. Chem*. B., 105 (2001) 6367–6374.
12. X. Lu, H. Zhang, L. Hu, C. Zhao, L. Zhang, X. Liu, *Electrochem. Commun*., 8 (2006) 1027-1034.
13. Y. Hirai, S. Sasaki, H. Tamiaki, S. Kashimura, Y. Saga, *J. Phys. Chem. B.*, 115 (2011) 3240-3244.
14. H. Jensen, J. J. Kakkassery, H. Nagatani, D. J. Fermín, H. H. Girault, *J. Am. Chem. Soc*., 122 (2000) 10943-10948.
15. D. Tamae, P. Lim, G. E. Wuenschell, J. Termini, *Biochemistry*, 50 (2011) 2321–2329.
16. M. M. Islam, T. Ohsaka, *J. Phys. Chem. C.*, 112 (2008) 1269-1275.
17. N. Eugster, D. J. Fermín, H. H. Girault, *J. Phys. Chem. B.*, 106 (2002) 3428-3433.
18. S. Wu, B. Su, *Chem. Eur. J.*, 18 (2012) 3169–3173.
19. H. Nagatani, D. J. Fermín, H. H. Girault, *J. Phys. Chem*. B., 105 (2001) 9463-9473.
20. S. Yoshimoto, A. Tada, K. Suto, R. Narita, K. Itaya, *Langmuir*, (2003) 19 672-677.
21. Y. Rio, G. Accorsi, N. Armaroli, D. Felder, E. Levillain, J. Nierengarten, *Chem. Commun.*, 10 (2002) 2830–2831.
22. X. Lu, M. Nan, H. Zhang, X. Liu, H. Yuan, J. Yang, *J. Phys. Chem*. C., 111 (2007) 14998-15002.
23. C. Shi, F. C. Anson, *Anal. Chem.*, 70 (1998) 3114-3118.
24. C. Shi, F. C. Anson, *J. Phys. Chem*. B., 102 (1998) 9850-9854.
25. M. Zhou, S. Gan, L. Zhong, X. Dong, *Phys. Chem. Chem. Phys.*, 14 (2012) 3659–3668.
26. C. Shi, F. C. Anson, *J. Phys. Chem*. B., 105 (2001) 1047-1049.
27. C. Shi, F. C. Anson, *J. Phys. Chem*. B., 105 (2001) 8963-8969.
28. D. Zigah, J. Noel, C. Lagrost, P. Hapiot, *J. Phys. Chem. C.*, 114 (2010) 3075–3081.
29. M. Shen, A. J. Bard, *J. Am. Chem. Soc.*, 133 (2011) 15737–15742.
30. P. Sun, F. Li, Y. Chen, M. Zhang, Z. Zhang, Z. Gao, Y. Shao, *J. Am. Chem. Soc*., 125 (2003) 9600-9601.
31. R.A. Marcus, *J. Phys. Chem*., 90 (1990) 1050-1055
32. R.A. Marcus, *J. Phys. Chem*., 94 (1990) 4152-4155.
33. R.A. Marcus, *J. Phys. Chem*., 95 (1991) 2010-2013.
34. M. Kubo, Y. Mori, M. Otani, M. Murakami, Y. Ishibashi, M. Yasuda, K. Hosomizu, H. Miyasaka, H. Imahori, S. Nakashima, *J. Phys. Chem. A.*, 111 (2007) 5136-5143.

35. J. Xu, A. Frcic, J. A. C. Clyburne, R. A. Gossage, H. Z. Yu, *J. Phys. Chem*. B., 108 (2004) 5742-5746.
36. A. Wahab, M. Bhattacharya, S. Ghosh, A. G. Samuelson, P.K. Das, *J. Phys. Chem. B.*, 112 (2008) 2842-2847.
37. R. E. Blankenship, *Molecular Mechanisms of Photosynthesis*. Blackwell Science (2002).
38. X. Q. Lu, L. N. Hu, X. Q. Wang, *Electroanalysis*, 17 (2005) 953-958.
39. X. H. Liu, L. N. Hu, L. M. Zhang, H. D. Liu, X. Q. Lu, *Electrochim. Acta*., 51 (2005) 467–473.
40. S. E. Ward Jones, F. G. Chevallier, C. A. Paddon, R. G. Compton, *Anal. Chem*., 79 (2007) 4110-9.
41. D. Zhan, S. Mao, Q. Zhao, Z. Chen, H. Hu, P. Jing, M. Zhang, Z. Zhu, Y. Shao, *Anal. Chem.*, 76 (2004) 4128-4136.